IET Research Journals

*Research Article*

IET Journals
The Institution of Engineering and Technology

ISSN 1751-8644
doi: 0000000000
www.ietdl.org

# Efficient modeling of IEEE 802.11p MAC output process for V2X interworking enhancement

*Fatma Salem*[1*], *Yassin Elhillali*[1], *Smail Niar*[1]

[1] *University of Valenciennes, CNRS, UMR 8201-LAMIH, F-59313 Valenciennes, France*
** E-mail: fatma.salem@univ-valenciennes.fr*

**Abstract:** Vehicle-to-anything (V2X) is a promising communication technology which expected to revolutionize the ground transportation system by improving traffic safety and efficiency for people on roads. The future deployment of V2X requires interworking between different access technologies, i.e., Dedicated Short-Range Communications (DSRC) and Cellular networks. However to achieve an efficient V2X interworking, we need to resolve the multi-hop issue, mainly originating from the V2X hybrid architecture. To resolve this issue and consequently to enhance the interconnected system, characterizing the output process of IEEE 802.11p-based DSRC MAC protocol is of a fundamental importance. This paper proposes Regenerative Model to provide a complete description of IEEE 802.11p output process. The accuracy of the model is verified through extensive simulations. As a case study, the proposed model is compared with Poisson model in the performance evaluation of V2X interworking. Numerical and simulation results verify the ability of the Regenerative Model to capture the deviations of the actual output process of IEEE 802.11p under different traffic intensity as compared to the Poisson model.

## 1 Introduction

There have been worldwide efforts from governments, academic institutions and industrial organizations under the big umbrella of Intelligent Transport Systems (ITS), to provide Vehicle-to-anything (V2X) communications. V2X is a promising communication technology with a great potential of supporting a variety of novel ITS applications to improve traffic safety and efficiency. As defined by the Third Generation Partnership Project (3GPP) group [1]., V2X is aiming to enable Vehicle-to Vehicle (V2V), Vehicle-to-Infrastructure (V2I) and Vehicle-to-Pedestrian (V2P) communications. An essential technology for realizing V2X communications is Dedicated Short-Range Communications (DSRC) which is achieved over reserved radio spectrum band allocated in the upper 5 GHz range [2]. The main enabling communication standard in DSRC is IEEE 802.11 which support V2V and V2I communications, the current version of the IEEE 802.11 standard incorporates the IEEE 802.11p amendment for Wireless Access in Vehicular Environments (WAVE), which is based on the ASTM E2213-03 standard for DSRC physical (PHY) and Medium Access Control (MAC) layer specifications. In IEEE 802.11p MAC different Quality of Service (QoS) classes are obtained by prioritizing the data traffic. Therefore, application messages are categorized into different Access Categories $ACs$, with $AC_0$ has the lowest and $AC_3$ the highest priority, where each $(AC)$ has different contention parameters to contend its packets for the shared communication channel [3].

Since the future deployment of V2X hybrid communications necessitates interworking between different access technologies, i.e, DSRC and cellular technologies, the issue of multi-hop packet transmission arises [4]. The multi-hop issue is defined as the capability of the mobile nodes (vehicles) to provide connectivity to a variety of access technologies in the interconnected hybrid network. The main challenge to resolve the multi-hop issue is that of characterizing the output process of IEEE 802.11p-based DSRC MAC protocol employed in the network mobile nodes. This output process is the input traffic process to the other nodes (i.e., cellular Base stations BSs and Road Side Units RSUs) in the interconnected network and affects considerably its operation.

The analytical tractability inherent to the memoryless Poisson model has tempted many researchers to adopt this model for the description of the interconnected network traffic processes; however, its validity for modeling the bursty real-time traffic has often been questioned [5]. In the high time-varying nature of vehicular networks we believe that the output process of IEEE 802.11p exhibits considerable changes under different traffic intensity, as the network induced packet delay is a function of the traffic intensity rate. On the other hand, as the traffic intensity increases, the output process flow tends to be bursty which makes the Poisson model unsuitable for modeling the output process of IEEE 802.11p. This claim is investigated in the following sub-section in detail.

### *1.1 Motivation*

The network induced packet delay is defined as the time difference between its generation time and the end of its successful transmission. The distance between two successful transmissions in the delay process constitutes the interdepature output process of IEEE 802.11p. The change in the traffic intensity has an impact on the network connectivity and on the likelihood of congestion on the shared communication channel which induces dynamics in the delay process of 802.11p mainly at high traffic intensity. In a high traffic scenario, the intensity of channel contention among the transmitted packets increases significantly due to a high transmission collision rate, resulting in a large induced packet delay. Since the interdeparture process is regenerative with respect to the delay process, the output interdeparture distribution will be affected by the changes in traffic intensity.

This effect of traffic intensity on the induced packet delay process and the regenerative interdepature process is visualized in Fig. 1. In this figure, one-dimensional vehicular network and a slotted shared communication channel with no propagation delays are considered. The input traffic rates in (packet/slot) are $\lambda = 0.1$ and $\lambda = 0.4$. The simulations were run for the four access categories $ACs$ each with its defined contention parameters. In the first Subfigure (a), the delay process is shown to be monotonically increasing with the traffic input rate. The delay for the $ACs$ is modestly increased at low rate, i.e., $\lambda = 0.1$ as the intensity of channel contention among the transmitted packets in not severe. As the input traffic rate increases, i.e., $\lambda = 0.4$, the induced delay is significantly increasing for each access category. The detailed Subfigures (b) and (c), show the clear impact

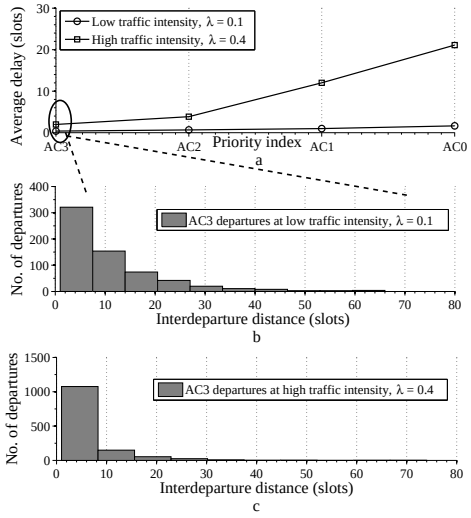


**Fig. 1**: Average packet delay and departure distribution.
*a* Average packet delay of different priority classes
*b* $AC_3$ departures distribution at low traffic intensity
*c* $AC_3$ departures distribution at high traffic intensity

of traffic intensity on the related interdepauture process for the high priority category $AC_3$. While Subfigure (b) exhibits an exponential distribution at low traffic rate, the interdepauture distribution seems to deviate further form the exponential distribution at high rate in Subfigure (c). From the latter Subfigure, it is interesting to note how the departures tend to group together at small range. This accumulation indicates the existence of burstiness as well as strong memory in the induced output process.

In such scenarios mentioned above and owing to the burstiness and memory charachteristics of IEEE 802.11p output process, the memoryless Poisson model is not suitable for the description of IEEE 802.11p-based DSRC output traffic. In order to resolve the multi-hop issue in V2X interworking, an accurate model for description of IEEE 802.11p output process should be developed that is able to capture the deviations in the output process under different traffic intensity.

### *1.2 Related Works*

Since IEEE 802.11p is the main communication standard which support V2V and V2I communications, also known as Vehicular Ad Hoc Networks (VANET), many analytical models and corresponding performance evaluations have been proposed in literature. The majority of these studies have focused on modeling the induced MAC protocol delay process and improving its throughput, the output process has only been considered in simulation results in terms of the packet reception rate or in departures' probability distribution. In general, modeling the output process of a MAC protocol is a much harder problem since it is intimately interwoven with the dynamical behavior of the algorithmic system of the protocol. Because of this fact, it is not surprising that results concerning the output process of IEEE 802.11p MAC characteristics are limited and obtained only through simulations, which are usually based on special assumptions [6, 7].

Early analytical methods for the IEEE 802.11p protocol were presented in the works of Torrent-Moreno *et al* [8, 9]. These works investigated critical information dissemination in 802.11p VANET. A performance evaluation using simulations and analytical means was then introduced in Eichler's work [10], where the capacity of the protocol to provide a reliable safety message dissemination was analyzed by considering beacon collision probability and delay. Apart from the collision probability and transmission delay, [11] investigated the influence of the beaconing generation rate on the probability of successful reception in IEEE 802.11p broadcasting mode.

Recent years, [12] proposed analytical model to evaluate the maximum stable throughput for unicast services in VANET. After that, Yao *et al* [13] introduced a Markovian analytical model, showing the performance of broadcast in terms of mean and deviation of MAC delay. Another Markovian model is proposed in [14] with limited retry limit to improve throughput and packet delay. One common factor is that the existing recent works are almost based on a Markovian model which usually gives insufficient information on the stability of 802.11p MAC protocol due to its scalability and hidden state issues.

Several works have studied the hybrid solutions that exploit the beneficial consequences of integrating DSRC and cellular technologies towards an efficient V2X communications. Vinel [15] provided a theoretical framework which compares the basic patterns of 802.11p and the cellular Long Term Evolution (LTE) technologies in the context of safety of life vehicular scenarios. The authors of [16] showed that broadcast, multicast modes can reduce the load on cellular downlink, while the uplink channel becomes a bottleneck in dense vehicular scenarios since the uplink transmissions are always achieved using unicast mode. In [17], the authors used a Markovian model evaluate the cellular LTE for safety services, where the data service user arrivals at the uplink was modeled to be Poissonian. In summary, the accurate performance evaluation of V2X communication solutions need to account for the actual DSRC output traffic, which is generally ignored in existing studies.

### *1.3 Main contributions*

This paper aims to present Regenerative Model to provide a complete description of IEEE 802.11p-based DSRC MAC output process, leading to traffic flow optimization in the future V2X communications. To our best knowledge available, there is no work that provides a complete model for the output process of IEEE 802.11p and its description. The main properties of the proposed model are summarized as follows:

- The model uses a powerful result from the theory of regenerative processes, in effect, to reduce the problem of defining a Markovian model to the problem of determining the steady-state interdeparture distribution of IEEE 802.11p output process.
- Due to its regenerative property, the model leads to define description models which provide complete description of 802.11p output process when employed under different traffic intensity.
- The model incorporates several design parameters in IEEE 802.11p including, MAC contention window size, packet generation rate and the service rate, so that important insights can be gained about IEEE 802.11p configuration and its functionality to support efficient V2X communications.
- As compared to the widely adopted Poisson model, the proposed Regenerative Model is superior in terms of ability and sensitivity to detect changes in IEEE 802.11p output process.

The above mentioned characteristics land Regenerative Model well to describe IEEE 802.11p output process in the future V2X interworking.

The rest of the paper is organized as follows: In Section 2, a review of 802.11 MAC algorithmic system and V2X hybrid architectures are given. In Section 3, the proposed Regenerative Model is detailed. The performance evaluation of the Proposed model is offered in Section 4. In Section 5, complete description models for the output process are defined. As a case study, in Section 6, Regenerative Model is incorporated in the evaluation of V2X interworking. Finally, the paper is concluded in Section 7.

## 2 IEEE 802.11P for V2X communications

### *2.1 Algorithmic system of 802.11p MAC in a Nutshell*

IEEE 802.11p uses the Enhanced Distributed Channel Access (EDCA) in ASTM E2213-03 standard as MAC method. The EDCA uses CSMA with collision avoidance (CSMA/CA) while prioritization is provided by using different channel access parameters for each packet priority. There are four available Access Categories

**Table 1** EDCA parameter set used for CCH

| $AC$ | $ACI$ | $CW_{min}$ | $CW_{max}$ | $AIFSN$ |
|---|---|---|---|---|
| Background | $AC_0$ | 15 | 1023 | 9 |
| Best effort | $AC_1$ | 7 | 125 | 6 |
| Safety | $AC_2$ | 3 | 7 | 3 |
| Safety of Life | $AC_3$ | 3 | 7 | 2 |

$ACs$ with $AC_0$ has the lowest priority and $AC_3$ the highest priority [3]. For each newly generated packet, the vehicle senses the shared Control Channel (CCH) activity before it starts the transmission. If the channel is sensed idle for a time period greater than or equal to a Distributed Inter-Frame Space (DIFS), the packet can be directly transmitted. If the channel is busy or becomes busy during the AIFS, the vehicle must wait unitl its backoff timer decreases to zero to be able to transmit again . The Backoff Timer (BT) value in 802.11p is chosen randomly from a discrete uniform distribution and drawn from a Contention Window (CW) with values from the interval $(0, CW_{min})$. For every retransmission attempt, the value of the BT will be doubled from its initial value until reaching $CW_{max}$ and the packet who reached the maximum number of attempts will be rejected out of the system. $CW_{min} = 15$ , $CW_{max} = 1023$ and a maximum number of seven attempts are the defined contention values in IEEE 802.11p. The contention parameters for CCH, adapted from [3], is shown in Table 1.

### *2.2 V2X hybrid architectures*

As an important first step toward the future V2X, fixed and dynamic hierarchical hybrid architectures have been proposed for V2X communications. In the fixed hierarchical architecture, the type of mobile nodes (e.g, public vehicles, private vehicles) belonging to each level of the hierarchy are preselected and do not change with time. In the dynamic hierarchy architecture, the network nodes are not defined based on their type and are assumed homogeneous which provid more flexibility and robustness to the network dynamics as compared to the fixed architecture [18]. One way to implement the dynamic architecture is by a clustering scheme, which groups vehicles into group of clusters. Each cluster has a Cluster Head (CH) that is responsible for maintaining the cluster and managing its resources. The other vehicles are called Cluster Members (CMs) which communicate with their CHs by using IEEE 802.11p. The CHs then aggregate the data collected from their CMs and transmit it to the static nodes in the network, i.e., cellular Base stations BSs and Road Side Units RSUs [18].

## 3 Regenerative Model for IEEE 802.11p

In this section, we develop Regenerative Model to compute the output traffic interdeparture distribution of IEEE 802.11p MAC protocol. Particularly, we find analytically the steady-state distribution of the distance between two consecutive successful transmissions. We consider a vehicular network with independent and identical (i.i.d) users. Time will be measured in slot units. The integer $T$ will denote slot indexes, slot $T$ occupies the transmission interval $(T, T + 1)$. In slot $T$ each user possesses the following attributes:

- The user generates a number $N_T$ of packets. The random variables $N_T$ are i.i.d with distribution

$$P(N_T = m) = P_m, \quad N_T \sim P_m(\eta_m, \sigma_m^2) \tag{1}$$

where $\eta_m$ and $\sigma_m^2$ are the finite mean and variance of the distribution respectively.
- Once a packet is generated the user will retain it in an infinite size buffer.
- As $m$ increases, $P_m$ converges to Poisson with rate $\lambda$ packets per slot.

Our methodology in developing the proposed model utilizes the regenerative character of the output process $\{\beta_i\}_{i\geq 1}$ that 802.11p MAC protocol generates. By observing the algorithmic system of 802.11p MAC as described in Subsection 2.1, it is relatively easy to identify the regeneration points at which the output process probabilistically restarts itself. If $\{R_i\}_{i\geq 1}$ represents a sequence of successive collision resolution time points on the most ending edges of slots containing successful transmissions and at which the lag equals one, then $\{R_i\}_{i\geq 1}$ is the sequence of the regeneration time points associated with output process $\{\beta_i\}_{i\geq 1}$. An important quantity in analyzing the proposed model is the Contention Resolution Interval (CRI) length. As described in Subsection 2.1, IEEE 802.11 MAC protocol utilizes a backoff value which is chosen randomly form a Contention Window ($CW$). The $CW$ values in Table 1 are defined so that the actual CRI length is $\leq CW$. As it will become clear later, the CRI length $L_m$ is determined by the number of collided packets in its first slot. The regenerative property of the induced output process leads to the following lemma

**lemma 1.** *If $d(n), n \geq 1$ is a discrete time process representing the distance between two consecutive successful transmissions in the output process $\{\beta_i\}_{i\geq 1}$ of IEEE 802.11p MAC algorithm, then there exist a random variable $d(\infty)$ such that the process $d(n), n \geq 1$ converges in distribution to $d(\infty)$. Given a sample function $\mathbb{1}_{\mathbb{n}}(r)$ of the process $d(n)$, then $d(\infty)$ represents the steady-state interdeparture distance induced by the algorithm and its distribution satisfies the equality*

$$P(d(\infty) = r) = \frac{1}{\lambda L_m} E\left\{\sum_{n=1}^{\tau_1} \mathbb{1}_{\mathbb{n}}(r)\right\}$$

*Proof:* Let the algorithmic system of IEEE 802.11p starts at time $T_0$ and define the sequence $\{R_i\}_{i\geq 1}$ such that $T_0 \leq R_1 \leq R_2 \leq \ldots$ to be the collision resolution time points on the most ending edges of slots containing successful transmissions and at which the lag equals one. Let $S_i, i \geq 1$ to be the number of successful transmissions in the interval $(T_0, R]$, $\forall R \in \{R_i\}_{i\geq 1}$ then

$$S_i = \sum_i 1(R_i \leq R) \quad \forall R \in \{R_i\}_{i\geq 1}; i \geq 1 \tag{2}$$

$S_i$ is a renewal counting process where the inter-renewal times $\zeta_j^i, \quad 1 \leq j < i$ are identically distributed random variables (i.i.d). If $d(n)$ denotes the distance between the $(n-1)\,th$ and the $n\,th$ successful transmission, then for the process $\{S_i, d_i(n)\}$ with inter-renewal times $\zeta_i^j$ the following regenerative theorem holds [19]

For the process $\{S_i, d_i(n)\}, \quad i \geq 1, n \geq 1$ with iner-renewal times $\zeta_j^i, \quad 1 \leq j < i$, its sample path $\tau_j$ in the time interval $(R_j, R_{j+1}]$ is described by:

$$\tau_j = \left(\zeta_j^i, d_j(n) \colon 1 \leq j < i, n \geq 1\right) \tag{3}$$

This $\tau_j$ is the $jth$ segment of the process which represents the number of successful transmissions in the interval $(R_i, R_{i+1}]$. Expression (3) states that, the process $d_i(n)$ is regenerative with respect to $S_i$. Hence the process $d(n)$ is regenerative over all the renewable points $\{R_i\}_{i\geq 1}$ as its segments $\tau_i, i \geq 1$ have lengths $l_i$ that are i.i.d. Giving that the sequence $\{\tau_i, i \geq 1\}$ is i.i.d, then

$$E\{l_i\} = E\{l_1\} = l \tag{4}$$

$$E\{\tau_i\} = E\{\tau_1\} = \Gamma \tag{5}$$

Where $l$ and $\Gamma$ are the mean segment length and throughput respectively. If the mean segment throughput is bounded, i.e.

$$\Gamma < \infty \tag{6}$$

Then from the renewal theory the following theorem holds [19]

For the discrete time process $d(n), n \geq 1$ which is regenerative with respect to $S_i, i \geq 1$ with $\tau_i$ as the $ith$ regeneration segment. If its sample function $\{f(d(n), n \geq 1)\}$ is a measurable nonnegative real-valued function then the function $\{f(d(n), n \geq 1)\}$ is also regenerative over all $\{R_i\}_{i\geq 1}$.

Define F to be the expected value of the sample function $\{f(d(n), n \geq 1)\}$ in the first segment $\tau_1$ such that

$$F = E\left\{\sum_{n=1}^{\tau_1} f\big(d(n)\big)\right\} < \infty \tag{7}$$

then, by invoking the law of large numbers the first equality in (8) holds with probability one. The expression in (8) shows how to establish the existence of the stationary distribution of the interdeparture process $d(n)$ by appropriately selecting the function $f$. Let us define $f\,(d(n))$ as the indicator function $\mathbb{1}_{\mathrm{n}}(r)$

$$\mathbb{1}_{\mathrm{n}}(r) = \begin{cases} 1, & \text{if } d(n) \leq r \\ 0, & \text{if } d(n) > r \end{cases} \tag{9}$$

This choice for the function $\mathbb{1}_{\mathrm{n}}(r)$ will permit the computation of the empirical distribution of $d(n)$, to see this let us rewrite (8) using (9)

$$\lim_{N\to\infty} \frac{1}{N} E\left\{\sum_{n=1}^{N} \Big\{\mathbb{1}_{\mathrm{n}}(r)\Big\}\right\} = \frac{1}{\Gamma} E \sum_{n=1}^{\tau_1} \Big\{\mathbb{1}_{\mathrm{n}}(r)\Big\} \tag{10}$$

At any fixed value of $r$, the expectation of the empirical distribution in (10) equals the cumulative distribution, which implies the existence of a real valued random variable $d(\infty)$ such that the sequence $d(n)$ converges in distribution to $d(\infty)$. Then, $d(\infty)$ is the steady-state of the interdeparture distance of the output process $\{\beta_i\}_{i\geq 1}$ with distribution defined as follows:

$$P(d(\infty) = r) = \frac{1}{\Gamma} E\left\{\sum_{n=1}^{\tau_1} \mathbb{1}_{\mathrm{n}}(r)\right\} = \frac{F}{\Gamma} \tag{11}$$

Thus, under the conditions stated in (6) and (7), the steady state distribution of the interdeparture process exist and its value is given in terms of the per segment parameters; the mean cumulative distance $F$ and mean segment throughput $\Gamma$.

## 4 Numerical Evaluation

In this Section we exploit the dynamics of the 802.11p MAC algorithmic system to evaluate the quantities $F$ and $\Gamma$ in (11).

### *4.1 Mean Segment Throughput*

The computation of the mean segment throughput $\Gamma$ in (11) depends on the input traffic rate $\lambda$; $\Gamma = \lambda l$, where $l$ is the expected value of segment length as defined in (4). Since the multiplicity of successive segments are i.i.d random variables, the expected segment length $l$ is approximating $L_m$ for sufficiently large $m$. $L_m$ is the expected value of the CRI length given that it starts with multiplicity of $m$ packets in the first slot, then

$$\Gamma = \lambda L_m \tag{12}$$

A proof of the last assertion is given in Appendix 9.1. In the following we compute the expected value of the CRI length.

**Table 2** Expected $CW$ length and the service rate

| $m$ | 0 | 1 | 2 | 3 | 4 | 5 | 6 | 7 |
|---|---|---|---|---|---|---|---|---|
| $L_m$ | 1 | 1 | 4.5 | 7 | 9.6 | 12.3 | 15 | 17.6 |
| $m/L_m$ | 0 | 1 | 0.44 | 0.428 | 0.416 | 0.406 | 0.4 | 0.397 |

*4.1.1 Expected value of CRI length:* Let $T$ corresponds to a starting slot of some CRI. Let $L_{m|n}$ to be the expected length of the CRI conditioned on having $n$ users with counter value 0. Then, from description of the algorithm the following equations hold

$$L_m = 1 \quad \text{for } m = 0, m = 1 \tag{13}$$

$$L_{m|n} = \begin{cases} 1 + L_n + L_{m-n} & \text{for } 1 \leq n \leq m \quad (14a) \\ 1 + L_m & \text{for } n = 0 \quad (14b) \end{cases}$$

Expression (14a) can be explained as follows: For $m \geq 2$, there is a collision in the first slot of the CRI, the 1 corresponds to the slot of the initial collision among the $m$ users. Then the CRI could be regarded as a partition of two subsets. The first subset is the expected number of slots needed to resolve the collision in slot 2 among $n$ users whose backoff timers decreased to zero. The probability that exactly $n$ users will transmit in slot 2 after the collision slot is

$$P_n = \binom{m}{n} 2^{-m} \tag{15}$$

The second subset is formed by the multiplicity of $(m - n)$ holding users whose backoff timers retained them form transmitting in slot 2, which will be initiated after the end of the previous subset. Expression (14b) results when none of the users in the initial collision has counter value 0, which occurs with probability $P_0$. Since

$$L_m = \sum_{n=0}^{m} L_{m|n} P_n \tag{16}$$

then, from (14a) and (14b) we obtain a finite dimensional linear system of the form

$$L_m = 1 + \sum_{n=0}^{m} \left(L_n + L_{m-n}\right) P_n - P_0 \tag{17}$$

Solving for $L_m$ we obtain the following recursion

$$L_m = \frac{1 + 2\sum_{n=0}^{m} L_n P_n - P_0}{1 - (2)^{1-m}}, \quad m \geq 2 \tag{18}$$

(18) represents the expected value of CRI length with initial conditions given by (13). Table 2 contains some of the computed values of $L_m$ along with the corresponding service rate $m/L_m$.

*4.1.2 Bounds on CRI length:* The computation of the quantity $\Gamma$ in (12) requires that $L_m$ to be finite for $m \geq 0$ and, moreover, it should be bounded. Our approach to determine bounds on $L_m$ is based on the observation of the coarse dependence of $L_m$ on $m$ as induced by (18). This observation allows us to assume that $m = 2m$ is very large, reformulating (14a) using this assumption gives

$$L_{2m} \approx 1 + 2L_m, \quad m >> 1 \tag{19}$$

Considering as an equality, (19) is a recursion whose solution is

$$L_m = \varepsilon m - 1, \quad m >> 1 \tag{20}$$

Since we assume that $m$ is very large, the desired upper bound for $L_m$ should guarantee a strictly positive service rate $(m/L_m)$.

$$\lim_{N\to\infty} \frac{1}{N} \sum_{n=1}^{N} \Big\{f\left(d(n)\right)\Big\} = \lim_{N\to\infty} \frac{1}{N} E\left\{\sum_{n=1}^{N} \Big\{f\left(d(n)\right)\Big\}\right\} = \frac{1}{\Gamma} E \sum_{n=1}^{\tau_1} \Big\{f\left(d(n)\right)\Big\} \tag{8}$$

If $(m/L_m) > 0$, then for every arrival rate that is smaller than $(m/L_m)$, the algorithmic system is stable. Hence the desired upper bound for $L_m$ should be of the form

$$L_m \leq \varepsilon_k m - 1, \quad m >> 1 \tag{21}$$

for an arbitrary positive integer $k$ such that $\varepsilon_k > 0$.

Table 1 shows that: $L_m - L_{m-1} \approx 2.7$ for $m \geq 3$. This indicates that the constant $\varepsilon_k$ in (21) is about 2.7. In Appendix 9.2 we proof that $L_m \leq 2.7m - 1$ can be optimized for best $\varepsilon_k$ value, so that

$$L_m \leq 2.68m - 1 \tag{22}$$

is tightly accurate for $m \geq 3$.

We note that the obtained value in (22) is closer to one obtained with the ALOHA-based binary protocol, this is true since IEEE 802.11p is a modified version of IEEE 802.11a which is ALOHA-based random access scheme [3].

Up to this point, $L_m$ and its upper bound have been calculated. The latter obtained values will be used to compute the mean segment throughput in (12). The objective is to evaluate the interdparture distribution in (11). As a last step before this evaluation, we calculate the mean cumulative interdparture distance over a segment $F$.

### *4.2 Mean cumulative distance over a segment*

In order to evaluate the mean cumulative interdeparture distance $F = E\left\{\sum_{n=1}^{\tau_1} \mathbb{1}_n(r)\right\}$, we need to compute the value of $\tau_1$, i.e., the number of packets that are successfully transmitted in the first segment. To that end, we first notice that the algorithm induces a sequence of consecutive CRIs. If $L_i$ denotes the length of the $i$th CRI, then from (18) the sequence $\{L_i\}_{1 \leq i < \infty}$ forms a Markove chain. The limiting distribution of the interdeparture distance in (11) fails to exist when this chain is periodic, hence for the chain to be aperiodic, the first segment should be in the first partition of the first CRI. To see this let use define the following quantities:

$L_d$ is the conditional expectation of the next CRI length, giving the length of the previous one equals $d$

$$L_d \triangleq E\left\{L_{i+1} \mid L_i = d\right\} \tag{23}$$

$P(m \mid d)$ is the probability that the number of packets (arrivals) at the beginning of the $(i+1)\,th$ CRI is $m$ given that the length of previous one is $d$. If the total number of the generated packets in the system is $M$ and the packet generating process as this in (1) then

$$P(m \mid d) = \binom{M}{m}(1 - P_1)^{(M-m)d}(P_1)^{md} \tag{24}$$

where $P_1$ is the probability of having single arrival in a slot time. Thus, the conditional expectation in (23) can be expressed as

$$\begin{aligned} L_d = \sum_{m=0}^{M} & E\left\{L_{i+1} \mid L_i = d, m \text{ arrivals at start of } L_{i+1}\right\} \\ & \times P(m \mid d) \end{aligned} \tag{25}$$

Since $E\left\{L_{i+1} \mid L_i = d, m \text{ arrivals at start of } L_{i+1}\right\} = L_m$, then

$$L_d = \sum_{m=0}^{M} L_m P(m \mid d) \tag{26}$$

For the markov chain $\{L_i\}_{1 \leq i < \infty}$ to be aperiodic, $P_1$ in (24) should be such that $P_1 > 0$ which implies that $\tau_1$ should lay on the first partition of $L_1$. (22) shows the linear growth of CRI mean $L_m$ with $m$, however its variance can also be proven (by analogous procedure to this we used to $L_m$) to grow linearly with the number of collision multiplicity $m$, hence by Markov's inequality, the $i\,th$ CRI length $L_i$ will be close to its mean $L_m$ with high probability for a sufficiently large $m$. As a result, the following clear bound on $\tau_1$ arises

$$1 \leq \tau_1 < S_n \tag{27}$$

where $S_n$ is the expected number of packets that are successfully transmitted in first partition of the CRI. To compute $S_n$ we must compute the rate of successful transmissions during the CRI. To that end, let $S_m$ be the expected number of packets that are successfully transmitted during CRI given that it started with $m$ packets and let $S_{m|n}$ be the expected number of packets that are successfully transmitted during the CRI conditioned on having $n$ packets in the first partition. Then, the operation of the algorithm yields the following relations for $S_{m|n}$:

$$S_{m|n} = \begin{cases} S_m & n = 0 \\ 1 + S_{m-1} & n = 1 \\ S_n & 2 \leq n \leq m \end{cases} \tag{28}$$

Denoting, as in (15), by $P_n$ the probability that $n$ arrivals occurred in an interval of length $L_n$, we have

$$S_m = \sum_{n=0}^{m} S_{m|n} P_n \tag{29}$$

Based on (28) and (29), we can write a recursion for $S_m$ with initial values $S_0 = 0, S_1 = 1$ as follows

$$S_m = \frac{(1 + S_{m-1})P_1 + \sum_{n=2}^{m-1} P_n S_n}{1 - P_0 - P_m}, \qquad m \geq 2 \tag{30}$$

### *4.3 Model Validation*

In order to verify the coarse dependence of the output process on the traffic intensity $\lambda$ as induced by (12). We report in Table 3 the analytically computed upper bounds $P_r$ on the distribution $P(d(\infty) = r)$ when the packet generation process is Poisson with rates $\lambda = 0.1, 0.3$ and $0.4$.

Since many traffic safety applications rely on the Beaconing mechanism, in which vehicles periodically broadcasting messages containing their current state (e.g., position, speed), we have developed a simulator in Matlab where each CM vehicle in the dynamic clustering scheme of Subsection 2.2 sends position Beaconing messages to its CH. This allows the CH to update and manage its cluster. The Beaconing messages generated according to Poisson process with different rates (0.1,0.3,0.4) which are within the required Beaconing generation rate specified in [11]. At the receiver CH, we observe the transmitted messages and we compute the interdeparture distance as the difference between two consecutive successful transmissions. We used $AC_3$ defined parameters from Table 1 to contend the messages for the CCH channel.

The obtained results from Table 3 and the simulation are graphically reported in Fig.2. From this figure we notice the following:

1. When the input rate is small, i.e., $\lambda = 0.1$, the interdeparture distance is approximately Geometrically distributed with $P_r \approx P(1 - P)^{(r-1)}$ where $P \approx \lambda e^{(-\lambda)}$.
2. As $\lambda$ gets larger, the interdeparure distribution tends to accumulate at relatively small values. For $\lambda = 0.3$ and $\lambda = 0.4$ we have $\sum_{r=1}^{12} P_r = 1$, which makes the output distribution in this case deviates further from the distribution in 1.

The above results demonstrate the ability of the proposed model to capture the deviations of the output process of IEEE 802.11p under different traffic intensity. A complete description of this process is essential in analyzing V2X interconnected systems as we will see later. Hence, the computation of the steady state interdeparture distance in Section 2 together with these results will be used to build description models for the actual output process of IEEE 802.11p.

**Table 3** Upper bounds on the interdeparture distribution

| | $\lambda = 0.1$ | $\lambda = 0.3$ | $\lambda = 0.4$ |
|---|---|---|---|
| $r$ | $P_r$ | $P_r$ | $P_r$ |
| 1 | 0.1443 | 0.2749 | 0.3781 |
| 2 | 0.0928 | 0.2268 | 0.2189 |
| 3 | 0.0825 | 0.1478 | 0.1517 |
| 4 | 0.0801 | 0.1065 | 0.0995 |
| 5 | 0.0722 | 0.0653 | 0.0522 |
| 6 | 0.0695 | 0.0378 | 0.0299 |
| 7 | 0.0619 | 0.0344 | 0.0274 |
| 8 | 0.0515 | 0.0275 | 0.0149 |
| 9 | 0.0513 | 0.0241 | 0.0075 |
| 10 | 0.0318 | 0.0240 | 0.0075 |
| 11 | 0.0309 | 0.0069 | 0.0050 |
| 12 | 0.0206 | 0.0068 | 0.0025 |

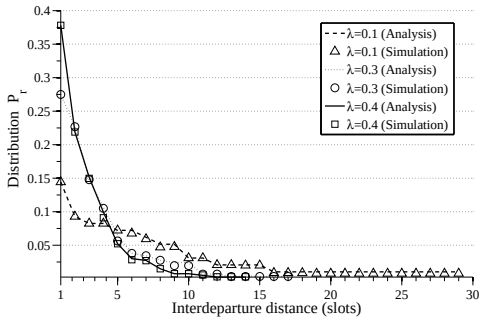


**Fig. 2**: Interdeparture distribution for different input traffic rates.

A procedure for the calculation of the parameters of the description models under different traffic scenarios is detailed in the following section.

## 5 Description of the output process

Since the (CCH) channel status process is in a direct interaction with the employed IEEE 802.11p, then the evolution of the channel status process determines completely the output process. This implies the following lemma, for which the proof is given in Appendix 9.3.

**lemma 2.** *Let $\{Ch_i\}_{i\geq 1}$ to be the status process of the shared channel CCH with a set of states $S = \{s_1, s_2, s_3\}$ such that $Ch_i \in S$ and define the output process $\{\beta_i\}_{i\geq 1}$ as a discrete binary process associated with slots of the channel CCH. Then, the output process can be considered as a two state channel status process*

$$\{\beta_i\}_{i\geq 1} = \{Ch_i\}_{i\geq 1} : Ch_i \in \{s_1, s_2\} \tag{31}$$

Lemma 2 shows that the meaningful procedure for the calculation of the parameters of the description models would be to equate their stochastic parameters to those in the actual output process where certain corresponding events occur.

### 5.1 The out put process in low traffic scenario

From Fig. 2 and for small input rates, the output distribution is close to the Bernoulli distribution. hence

$$\{\beta_i\}_{i\geq 1} \sim \text{Brn} = \begin{cases} P(\beta_i = s_1) = P \\ P(\beta_i = s_2) = 1 - P \end{cases} \tag{32}$$

The only parameter of the Bernoulli description model in (32) is $P$ which is equal to the probability of a successful packet transmission in the actual output process. The probability of success equals the packet input rate under stable algorithmic operation. Hence, the interdeparture distance distribution is given by

$$P_r = P(1-P)^{(r-1)} \tag{33}$$

### 5.2 The out put process in high traffic scenario

In a high traffic scenario, the traffic rate is heavy and bursty, hence IEEE 802.11p introduces strong dependency among the consecutive slots. As a result, we expect the IEEE 802.11p to generate an output traffic with memory. In fact, the accumulation in the interdeparture distribution for $\lambda = 0.4$ in Fig. 2 puts into evidence the memory feature of the actual output process. One way to capture this memory, would be describing the resulting process by a First-Order Markov Process (FOMP) whose parameters related to those of the actual output process. Since the actual output process is to be described by FOMP with parameters $\lambda$ and $\boldsymbol{b}$; $\lambda$ is the traffic rate and $\boldsymbol{b}$ is traffic burstiness coefficient, then it is suitable to work on the steady state distributions. From Lemma 2, if $\Pi(s_1), \Pi(s_2)$ are the steady state probabilities of the channel status process $\{Ch_i\}_{i\geq 1}$ in state $s_1$ and $s_2$ respectively, then under the stable algorithmic operation, it is evident that $\Pi(s_1) = \lambda$ and $\Pi(s_2) = 1 - \lambda$. The FOMP transition probabilities are given by

$$P(s_1 \mid s_1) = 1 - P(s_2 \mid s_1) \tag{34}$$

$$P(s_2 \mid s_2) = 1 - P(s_1 \mid s_2) \tag{35}$$

By invoking Bayes' theorem, we have

$$P(s_2 \mid s_1) = \frac{P(s_2, s_1)}{\Pi(s_1)} \tag{36}$$

$$P(s_1 \mid s_2) = \frac{P(s_2, s_1)}{\Pi(s_2)} \tag{37}$$

The burstiness coefficient $\boldsymbol{b}$ is defined by

$$\boldsymbol{b} = P(s_1, s_1) - P(s_2 \mid s_1) \tag{38}$$

In order to evaluate the above transitional probabilities we need to find the joint probability $P(s_2, s_1)$. From the description of the algorithm it is evident that a CRI which is ending with a successful transmission is followed by an idle slot. This gives rise to a joint pair $(s_2, s_1)$ of successive slots in the channel statues process

$$P(m_{i+1} = 1 \mid m_i = m) = P(s_2, s_1) \tag{39}$$

$P(m_{i+1} = 1 \mid m_i = m)$ takes the general form

$$\begin{aligned} &P(m_{i+1} = \acute{m} \mid m_i = m) = \\ &\sum_{l=1}^{\infty} P(m_{i+1} = \acute{m} \mid L_i = l) P(L_i = l \mid m_i = m) \end{aligned} \tag{40}$$

The first term on the right hand side of the equality (40) is the conditional probability of the $(i+1\,th)$ CRI with multiplicity $m_{i+1}$, given that the expected length of the $i\,th$ CRI is $l$. The second term is the conditional probability of the $i\,th$ CRI. Given a Poisson arrival process of rate $\lambda$ and for $\acute{m} = 1$, (40) can be rewritten as

$$\begin{aligned} &P(m_{i+1} = 1 \mid m_i = m) = \\ &\sum_{l=1}^{\infty} (\lambda l)\, e^{-\lambda l}\, P(L_i = l \mid m_i = m) \end{aligned} \tag{41}$$

Because of (13), $P(L_i = l \mid m_i = m) = 1$ for $m_i = 0, 1$. From (18) and Table 2, it can be seen that every odd number is a possible value of $L_i$, hence $P(L_i = l \mid m_i = m)$ could be written as

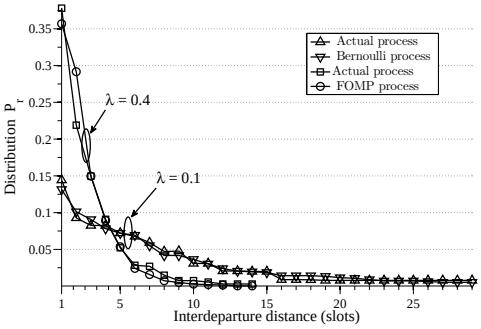


**Fig. 3**: Actual, Bernoulli and FOMP at low and high traffic rates.

$$P((2N+1) \mid m_i = m), m \geq 2 \tag{42}$$

Computing (42) for $m = 2$ is sufficient for the joint probability pair $P(s_2, s_1)$. With $m = 2$, we have $P((2N+1) \mid 2) = 2^{-N}, N \geq 1$, hence in view of (41) with $m = 2$, the desired joint probability in (39) is given by

$$\begin{aligned} P(m_{i+1} = 1 \mid m_i = 2) &= \sum_{N=1}^{\infty} \lambda(2N+1)e^{-\lambda(2N+1)}2^{-N} \\ &= \frac{3}{2}\,\lambda\, e^{-3\lambda} \end{aligned} \tag{43}$$

The transitional probabilities of FOMP model is then calculated form (36) and (37) and since the steady state probabilities are also computed, the description FOMP output process is completely determined.

**Remark 1.** *Let $P_{\acute{m}m} \triangleq P(m_{i+1} = \acute{m} \mid m_i = m)$. Then, $P_{10} = \lambda e^{-\lambda}$ is the parameter of Bernoulli output process, as noted from Fig.* 2. *In the actual output process and for small input rates, single arrivals in two successive slots occur with probability $P_{10}^2 \approx \lambda^2$ while the probability to have a collision slot $P_{21}$ is then equals to $\frac{1}{2}\lambda^2 e^{-\lambda} \approx \frac{1}{2}\lambda^2$. This explains the increase in the interdeparture distance probability $P_r$ for $r = 1$ above the Bernoulli parameter $P_{10}$.*

### *5.3 Evaluation of the description models*

In this Subsection, we evaluate the accuracy of the description models using the same simulation scenario of Subsection 4.3. Fig. 3 shows the actual interdepatrure process and the description interdepatrure processes for low and high traffic scenarios. The figure shows how the interdeparture distribution is close to Bernoulli at low input rates, it also shows that the FOMP provides a good description for the output process as the input rate increases. A more detailed examination of Bernoulli description model is depicted in Fig. 4. The figure shows how the pdf and cdf of the interdeparture distance in Bernoulli process are well fitted to the actual output process. In Fig. 5, we plot the system transition probabilities $P_{\acute{m}m}$ of the actual process along with those computed analytically from FOMP description process. From the figure we see how the joint probability increases with the input rate, however for rates above $0.4$ the joint probability starts to decrease. This is due to the fact that for high rates IEEE 802.11p introduces strong dependency but as the input rate increases above $0.4$ the packet rejection rate increases leading to a drop in the joint probability. The latter increase in the rejection rate is due to the increase in the collision probability $P_{21}$ for which the corresponding transition probability $P_{12}$ increases as well with the increasing input rate. Most importantly, however, we can see that there is good agreement between the transition probabilities of FOMP and the actual system.

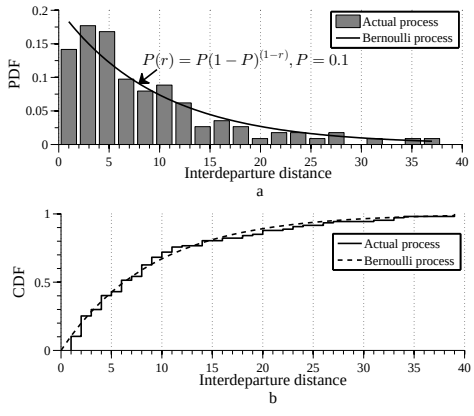


**Fig. 4**: Bernoulli interdeparture process vs. actual process.
*a* probability density function (PDF)
*b* cumulative distribution function (CDF)

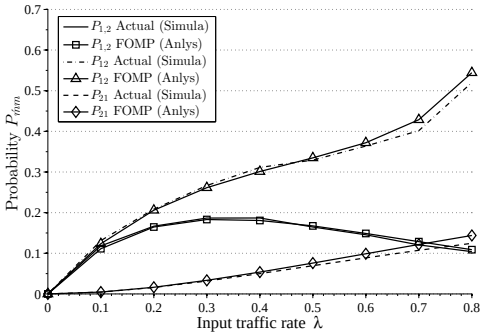


**Fig. 5**: System probabilities $P_{\acute{m}m}$ vs. input traffic rate $\lambda$.

## 6 V2X Application Scenario

In this section the output traffic modeling and the corresponding results presented before are incorporated in the performance evaluation of V2X interworking in the dynamic clustering scheme of Subsection 2.2. Particularly we focus on the associated message uplink form CHs to a cellular base station (BS) where each input flow to the BS represents an output process from the employed 802.11p in each cluster. The mean uplink delay $D$ is an essential measure of the performance of V2X interworking. In order to derive $D$ a queuing model has been applied to the uplink path of the BS. More specifically, we consider a queuing traffic model with $M$ cluster flows, $\lambda_j$ be the $jth$ cluster output rate in (packets/slot). Since we assume a slotted time system with fixed$-$length data packets, then the same constant amount of service will be required at the base station which implies that the input (output) processes $\{\beta_i^j\}_{i\geq 1}, j = 1, 2, \ldots, M$ are synchronized.

If the interworking is within a small number of clusters, then the employed IEEE 802.11p works in a low traffic scenario. In this case, the output process is Bernoulli process. Thus using Queuing Theory [20], the average number of packets $S_B$ in the cellular uplink is given by

$$S_B = \frac{\sum_{j=1}^{M}\sum_{k>j}^{M}\lambda_j\lambda_k + \Lambda(1-\Lambda)}{1-\Lambda} \tag{44}$$

where

$$\Lambda = \sum_{j=1}^{M}\lambda_j \tag{45}$$

From the well known Little theorem, the mean packet delay, $D_B$ is given by

$$D_B = S_B/\Lambda. \tag{46}$$

As the number of the clusters increases, the resulted output process form the employed 802.11p is FOMP. The average number of

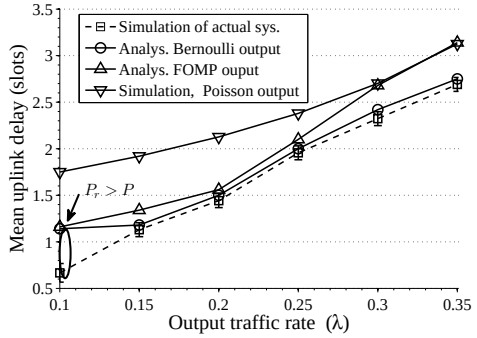


**Fig. 6**: Mean uplink delay as a function of the output rate, $M = 3$.

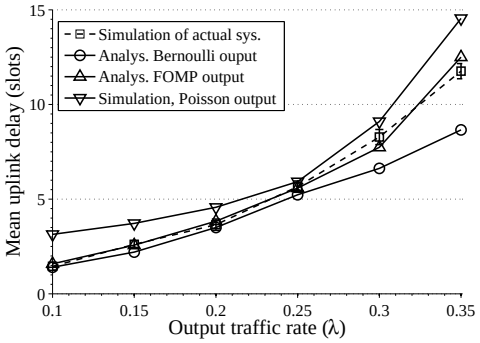


**Fig. 7**: Mean uplink delay as a function of the output rate, $M = 5$.

packets $S_K$ in this case is

$$S_K = \Lambda + \frac{\sum_{j=1}^{M}\sum_{k>j}^{M}\lambda_j\lambda_k\left[1+\frac{\boldsymbol{b}_j}{1-\boldsymbol{b}_j}+\frac{\boldsymbol{b}_k}{1-\boldsymbol{b}_k}\right]}{1-\Lambda} \quad (47)$$

where $\boldsymbol{b}$ is the burstiness coefficient as defined in (38)
Then, the mean packet delay $D_K$ is given by

$$D_K = S_K/\Lambda. \quad (48)$$

The induced mean uplink delay was computed from the expressions above for $M = 3$ and $M = 5$. The obtained values are shown in the Figures 6 and 7 along with the values resulted from simulating the actual queuing system. Fig. 6 shows that both of the output description models perform well as the queuing problem is not significant when $M = 3$. Even though the delay induced in the Bernoulli model for $\lambda = 0.1$ is relatively high, its performance outperforms Markov as the output rate increases, i.e., $\lambda \geqslant 0.3$. In fact, the Bernoulli model induced delay is more closer to the actual system delay. The increase in the Bernoulli delay for $\lambda = 0.1$ is due to the fact that the Bernoulli output process has interdeparture probability $P_r$ at $r = 1$ which exceeds its mean parameter $P$ as explained in Remark 1. As expected for $M = 5$, FOMP performs better than Bernoulli. This is clearly shown in Fig. 7 as the actual system induced delay is closer to the induced delay under FOMP model since the latter captures some of the dependency introduced by the algorithmic system of IEEE 802.11p. The interworking induced average packet delay is shown in Fig. 8; it is the average time between the packet generation time and the end of its successful transmission. It is provided here to indicate the total average delay that the packet undergoes in the cluster network and the uplink path. As expected from the previous results the induced total average delay is less when $M = 3$, as compared to $M = 5$.

As we mentioned in the beginning, due to its tractability the Poisson model is generally adopted to model the interconnected network traffic processes. We compared our Regenerative Model with the Poisson model in the evaluation of V2X interworking scheme discussed in the beginning of this section. As clearly shown form the

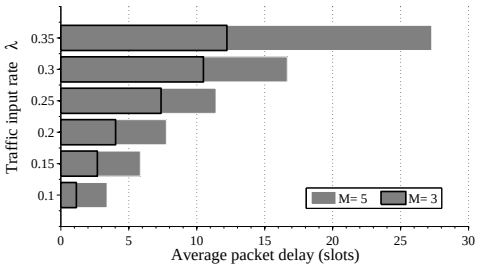


**Fig. 8**: The total interworking average packet delay.

results in Fig. 6 and Fig. 7, the performance of the Regenerative Model is superior to that of Poisson because the latter fails to capture the real variations in the traffic intensity. Our results show clearly that the adoption of Poisson model results in erroneous packet delay calculations which lead to inaccurate identification of the bottlenecks in V2X interworking.

## 7 Conclusion

In this paper, we presented Regenerative Model to completely describe the output process of IEEE 802.11p MAC protocol. The model incorporates different design parameters of IEEE 802.11p, so that important insights can be gained about the capability of 802.11p to provide efficient V2X interworking. The analytical results verified through extensive simulations show the accuracy of the proposed model in describing the actual output process of IEEE 802.11p. Moreover, the proposed model is compared with the Poisson model in the performance evaluation of V2X interworking. As compared to Poisson model, the proposed model ability to capture the deviations of the actual output process of IEEE 802.11p when employed under different traffic intensity is superior to that of Poisson model.

## 8 References

[1] 3GPP., 'Study on LTE-Based V2X Services (Release 14), Tech. Specification Group Serv. Syst. Aspects (TSG SA)', (3GPP TR, 2016)

[2] Harding, J. Powell, G., Yoon, R., et al.: 'Vehicle-to-vehicle communications: Readiness of V2V technology for application',(NHTSA, 2014), pp. 1-327

[3] IEEE., 'IEEE Standard for Wireless Access in Vehicular Environments (WAVE)-Multi-Channel Operation', (IEEE Std 1609.4, 2016), pp. 1-94

[4] Abboud, K., Aboubakr Omar, H., Zhuang, W.: 'Interworking of DSRC and Cellular Network Technologies for V2X Communications: A Survey', IEEE Transactions on Vehicular Technology, 2016, 1, (2), pp. 1-7

[5] Paxson, V., Floyd, S., 'Wide area traffic: the faliure of Poisson modeling', IEEE/ACM Trans. Networking, 2015, 3, pp. 226-244

[6] Campolo, C., Molinaro, A., Vinel, A., et al.: 'Modeling Prioritized Broadcasting in Multichannel Vehicular Networks', IEEE Transactions on Vehicular Technology, 2012, 61, (2), pp. 687-701

[7] Khan, S., Alam, M., Mllner, N., et al.:, 'A hybrid MAC scheme for emergency systems in urban VANETs environment', IEEE Vehicular Networking Conference (VNC), Columbus, OH, 2016, pp. 1-2

[8] Torrent-Moreno, M., Mittag, J.: 'Adjusting Transmission Power and Packet Generation Rate of Periodic Status Information Messages in VANETs', Proc. of the third ACM International Workshop on Vehicular Ad Hoc Networks, CA, Sep., 2006, pp. 90 - 91

[9] Schmidt-Eisenlohr, F., Torrent-Moreno, M ., Mittag, J., et al.: 'Simulation Platform for Inter-Vehicle Communications and Analysis of Periodic Information Exchange', Proc. of the 4th Annual IEEE/IFIP Conference on (WONS), Obergurgl, Austria, Jan., 2007

[10] Eichler, S.: 'Performance Evaluation of the IEEE 802.11p WAVE Communication Standard', IEEE 66th Vehicular Technology Conference, Baltimore, 2007, pp. 2199-2203

[11] Vinel, A., Staehle, D., Turlikov, A.: 'Study of Beaconing for Car-to-Car Communication in Vehicular Ad-Hoc Networks', IEEE International Conference on Communications Workshops, Dresden, 2009, pp. 1-5

[12] Etemadi, N., Ashtiani, F.: 'Throughput analysis of IEEE 802.11-based vehicular ad hoc networks', IET Communications, 2011, 5, (14), pp. 1954-1963

[13] Yao, Y., Rao, L., Liu, X., et al.: 'Delay analysis and study of IEEE 802.11p based DSRC safety communication in a highway environment', Proc. IEEE INFOCOM, Turin, 2013, pp. 1591-1599

[14] Cao, S., Lee, V.: 'Improving throughput of multichannel MAC protocol for VANETs', ICVES, Beijing, 2016, pp. 1-6

[15] Vinel, A.: '3GPP LTE Versus IEEE 802.11p/WAVE: Which Technology is Able to Support Cooperative Vehicular Safety Applications?', IEEE Wireless Communications Letters, 2012, 1, (2), pp. 125-128

[16] Calabuig, J., Monserrat, J., Gozalvez, D., et al.: 'Safety on the roads: LTE alternatives for sending ITS messages', IEEE Veh. Technol. Mag., 2014, 9, (4), pp. 6170

[17] Li, W., Ma, X., Wu, J., et al.: 'Analytical Model and Performance Evaluation of Long-Term Evolution for Vehicle Safety Services', IEEE Transactions on Vehicular Technology, 2017, 66, (3), pp. 1926-1939

[18] Ucar, S., Coleri S., Ozkasap, O.: 'Multi-hop cluster based IEEE 802.11p and LTE hybrid architecture for VANET safety message dissemination', IEEE Trans. Veh. Technol., 2015, 65, (4), pp. 2621-2636

[19] Breuer, L., Dieter, B.: 'Renewal Theory', in An Introduction to Queueing Theory and Matrix-Analytic Methods, (Springer, 2005)

[20] Ralph, L., Disney, T., Ott, J.: 'Networks of Queues', in Applied Probability-Computer Science: 'The Interface' (Springer Science and Business Media, 1982)

## 9 Appendices

### *9.1 Proof of the assertion given in (12)*

Let us define

- $CW$: The contention window size.
- $P_m(\eta_m, \sigma_m^2)$: The distribution of the traffic formed by the arrival packets with mean $\eta_m$ and variance $\sigma^2$.
- $P$: The probability that a single transmission occurring in an interval of expected length $l$.
- $\lambda$ : Poisson arrival rate.
- $S$ : The expected number of successful packets in a CRI of expected length $L$.

Let $m$ represents the total number of arrivals in the interval $l$ with rate $\eta_m$. If the contention resolution, induced only a single successful transmission in the interval $l$, then the probability $P = CW/\,l$. However, under stable operation of the algorithmic system ($m$ is small), the probability of having a single packet is also equals the input rate , i.e., $P = \eta_m$. Now let $m$ to increase and the quantities $\eta_m$ and $\sigma^2$ in the arrivals' distribution $P_m$ simultaneously to decreases so that

$$\eta_m m = \lambda \qquad \text{for } \lambda > 0, m >> 1 \tag{49}$$

the latter expression is the Poisson theorem, then $P_m$ converges in distribution to Poisson process, i.e., $P_m \longrightarrow Pois(\lambda)$.
Since $P = \eta_m$ and $\eta_m \triangleq m/l$, then (49) can rewritten as

$$CW/\,l \cdot \eta_m l = \lambda \tag{50}$$

In Poisson process, the arrival points in an interval is uniformly distributed. Hence, if a fraction $S/\lambda CW$ of the packets are successfully transmitted in a CRI it means that $S/\lambda CW$ is the fraction of the interval resolved. Therefore, $(S/\lambda CW)CW = S/\lambda$ represents the average portion of the resolved interval, which takes on the average $L$ slots to be resolved. Thus, in view of the CRI recursion in (18), the algorithm remains stable, even when it is highly loaded ($m$ is large), whenever it is able to resolve collisions at the rate in which the arrival process progresses in time, i.e.,

$$L = \frac{S}{\lambda} \tag{51}$$

Substitution of (50) and rearranging

$$L = \left(\frac{S}{\Gamma}\right) l \tag{52}$$

$\Gamma$ is the expected number of successful transmissions in the interval $l$

The random sequence $\{\tau_i, i \geq 1\}$ in (5), is i.i.d with common finite mean, i.e., $E\{\tau_i\} = \Gamma$. If we were to observe the values $\tau_1, \tau_2, \ldots$ in time till a random time point $N$, then from the algorithmic operation the following equality holds

$$S_N = \sum_{i=1}^{N} \tau_i$$

$S_N$ is total number of successful transmissions observed till the random stopping time $N$.

Let $T_N \triangleq \sum_{i=1}^{N} E\{\tau_i\}$, then by Wald's theorem

$$E\{S_N\} = E\{T_N\} \tag{53}$$

$$S = \Gamma \tag{54}$$

The last equality is in the stopping time sense and consequently (12) holds.

### *9.2 Bounds on the expected value of CRI length*

In (21), we seek the smallest value for the constant $\varepsilon_k$ for which the latter bound is true. The point of departure is the Kronecker delta function $\delta_{i,j}$ defined as

$$\delta_{i,j} = \begin{cases} 1, & \text{if } i = j \\ 0, & \text{if } i \neq j \end{cases} \tag{55}$$

using (55), the inequality in (21) can be rewritten as

$$L_m \leq \varepsilon_k m - 1 + \sum_{n=0}^{k-1} \delta_{n,m}(L_m - \varepsilon_k m + 1) \tag{56}$$

$$L_m \leq \varepsilon_k m - 1 + (L_m - \varepsilon_k m + 1) \tag{57}$$

Since, the right hand side of (57) equals $L_m$, then substituting the obtained bound from (56) in (18) we get

$$L_m \leq \frac{\varepsilon_k m - 1 - P_0 + 2\left[\sum_{n=0}^{k-1}\left(L_n - \varepsilon_k n + 1\right)P_n\right]}{1 - (2)^{1-m}} \tag{58}$$

observing (58), it can be seen that (21) holds if we choose $\varepsilon_k$ such that the summation quantity in (58) is non positive for $m \geq k$, i,e.,

$$\sum_{n=0}^{k-1} \Big( L_n - \varepsilon_k n + 1 \Big) P_n \leq 0 \tag{59}$$

$$\varepsilon_k \sum_{n=0}^{k-1} n P_n \geq \sum_{n=0}^{k-1} (L_n + 1) P_n \tag{60}$$

thus the required $\varepsilon_k$ is given by

$$\varepsilon_k \geq \left[ \frac{\sum_{n=0}^{k-1} (L_n + 1) P_n}{\sum_{n=0}^{k-1} n P_n} \right] \tag{61}$$

For the computation of (21) we assumed that $m$ is very large such that $\varepsilon_k \geq (L_m + 1)/m$. Therefore (61) represents the supremum from which we can obtain the smallest $\varepsilon_k$

$$\varepsilon_k = \max \left( (L_m + 1)/m, \sup_{m \geq k} \left[ \frac{\sum_{n=0}^{k-1} (L_n + 1) P_n}{\sum_{n=0}^{k-1} n P_n} \right] \right) \tag{62}$$

For a given $m$, the value of $L_m$ can be computed from (18), see Table 2, and hence determine $\varepsilon_k$ as in (62). Thus it is a simple matter numerically to find that for $m \geq 3$, we have

$$L_m \leq 2.68m - 1 \tag{63}$$

**Remark 2.** *The obtained upper bound in (*63*) guarantees a positive service rate $m/L_m$ for the stability of the algorithmic system as claimed in Subsection* 4.1.2*. To show this, we start with the fact that the expression in (*61*) represents the supremum. Hence the Poisson approximation is valid, then asymptotically, we have $\sum_{n=0}^{k-1}(L_n P_n) \approx L_m$ and $\sum_{n=0}^{k-1}(n P_n) \approx \lambda L_m$. Using the latter approximations, the inequality in (*61*) can be written as*

$$\varepsilon_k \geq \left[ \frac{L_m + 1}{\lambda L_m} \right] \tag{64}$$

*Since $m/L_m = \lambda \quad as \quad m \to \infty$ , then*

$$\frac{m}{L_m} \geq \frac{1}{\varepsilon_k} + \frac{1}{\varepsilon_k L_m} \qquad m \geq k \tag{65}$$

*Hence the service rate $m/L_m$ is guaranteed to be larger than $1/\varepsilon_k$, if the arrival rate is smaller than the latter service rate, then the algorithm is stable.*

### *9.3 Proof of lemma 2*

Given $m$ and $\eta_m$ as in (1), the quantity $\mu = m\eta_m$ is the input rate of the logarithmic system. Define the output rate $\alpha$ such that $\alpha = \frac{1}{n} \sum_{i=1}^{n} \beta_i$, where $\beta_i = 1$ if the $i\,th$ slot is a success slot, i.e., one user transmitting and $\beta_i = 0$ otherwise. If $\overset{\star}{\lambda}$ is the system throughput, then the following simple throughput definition relates the output process with the channel status process

$$\overset{\star}{\lambda} = \sup \big( \mu \colon \mu = \alpha \big) \tag{66}$$

(66) implies that the channel is noiseless which is by definition allows us to partition the channel output into disjoint sets. Hence, the shared channel (CCH) at slot $T$ can be viewed in one of the following status: $s_1$ if only one user is transmitting at $T$, $s_2$ if more than one user transmitting at $T$ hence a collision occurs and $s_3$ is idle if no user occupying the channel at $T$. Since the last two states do not result in an output, we can lump them both in one state $s_2$ and consider the channel status process as a two state process.

Since $\alpha = \frac{1}{n} \sum_{i=1}^{n} \beta_i$ and in viewing the noiseless channel mapping in (66), the output process $\{\beta_i\}_{i \geq 1}$ and a two state channel status process $\{Ch_i\}_{i \geq 1}, Ch_i \in \{s_1, s_2\}$ are identical, hence

$$\{\beta_i\}_{i \geq 1} = \{Ch_i\}_{i \geq 1} \, : Ch_i \in \{s_1, s_2\}$$

We note that the throughput definition in (66) applies for the infinite population model, $m$ is large, as well. Hence we could have specified $\mu = \lambda$, where $\lambda$ is Poisson input rate, in (66) and the Lemma would still hold.